TBC1D24 regulates recycling of clathrin-independent cargo proteins mediated by tubular recycling endosomes

Nguyen Thi Kim Nguyen, Norihiko Ohbayashi, Yasunori Kanaho*, Yuji Funakoshi*

Department of Physiological Chemistry, Faculty of Medicine and Graduate School of Comprehensive Human Sciences, University of Tsukuba, 1-1-1 Tennodai, Tsukuba, Ibaraki 305-8575, Japan.

*Correspondence to: Yuji Funakoshi or Yasunori Kanaho

Department of Physiological Chemistry, Faculty of Medicine and Graduate School of Comprehensive Human Sciences, University of Tsukuba, 1-1-1 Tennodai, Tsukuba 305-8575, Japan

Tel: (+81) (+81) 29-853-3115 (YF) or 29-853-3282 (YK)

Fax: (+81) 853-3271

E-mail: funa@md.tsukuba.ac.jp (YF) or ykanaho@md.tsukuba.ac.jp (YK)

Abstract

Many plasma membrane proteins enter cells by clathrin-independent endocytosis (CIE). Rab family small GTPases play pivotal roles in CIE and following intracellular trafficking of cargo proteins. Here, we provide evidence that TBC1D24, which contains an atypical Rab GAP domain, facilitates formation of tubular recycling endosomes (TREs) that are a hallmark of the CIE cargo trafficking pathway in HeLa cells. Overexpression of TBC1D24 in HeLa cells dramatically increased TREs loaded with CIE cargo proteins, while deletion of *TBC1D24* impaired TRE formation and delayed the recycling of CIE cargo proteins back to the plasma membrane. We also found that TBC1D24 binds to Rab22A, through which TBC1D24 regulates TRE-mediated CIE cargo recycling. These findings provide insight into regulatory mechanisms for CIE cargo trafficking.

Key words

clathrin-independent endocytosis, small GTPase, TBC1D24, tubular recycling endosomes, Rab22A

Abbreviations (non-standard or uncommon abbreviations)

CME: Clathrin-mediated endocytosis

CIE: Clathrin-independent endocytosis

TRE: Tubular recycling endosome

EE: Early endosome

SE: Sorting endosome

EEA1: Early endosome antigen 1

ERC: Endocytic recycling compartment

GEF: Guanine nucleotide exchange factors

GAP: GTPase-activating proteins

TBC: Tre2/Bub2/Cdc16

Tf/TfR: Transferrin/Transferrin receptor

MHCI: Major histocompatibility complex class I

CD98: Cluster of differentiation 98

Introduction

Endocytosis is a fundamental process internalizing extracellular materials and plasma membrane components, which are transported to lysosomes for degradation or to other organelles, or recycled back to the plasma membrane. There are two major types of endocytosis, clathrin-mediated endocytosis (CME) and clathrin-independent endocytosis (CIE) [1,2]. Although CME and the following intracellular trafficking pathways have been extensively studied, much less is known about the molecular mechanism of CIE.

Recent studies have proposed a model for the post-endocytic trafficking of CIE cargo proteins in HeLa cells [1,3-5]. Conventional CIE cargo proteins, such as MHCI and CD59, are internalized into vesicles that fuse with early endosomes (EE)/sorting endosomes (SE) associated with Rab5 and the early endosome-associated antigen 1 (EEA1). These cargo proteins are then sorted to lysosomes for degradation or recycled back to the plasma membrane via the endocytic recycling compartment (ERC) and tubular recycling endosomes (TREs), which are a hallmark of the CIE cargo trafficking pathway. On the other hand, the recent studies have identified a new set of CIE cargo proteins, including CD44, CD98 and CD147, following the distinct trafficking pathway [6-8]. After internalization, these cargo proteins are predominantly sorted away from EEA1-containing endosomes and directly transported to TREs, preventing them from targeting to lysosomal degradation. Various small GTPases including Rab5, Rab11, Rab22, Rab35, and Arf6 are involved in CIE cargo trafficking [6,7,9-14]. Activity of small GTPases is regulated by guanine nucleotide exchange factors (GEFs) and GTPase-activating proteins (GAPs): the conversion from the GDP-bound inactive form to the GTP-bound active form is accelerated by GEFs, and hydrolysis of GTP by the small GTPase is activated by GAPs [15-17]. Although there are multiple GEFs and GAPs for Rabs and Arf6, only a limited number of GEFs and GAPs are identified as regulators of CIE cargo trafficking [15-17].

TBC1D24 is characterized by a Tre2/Bub2/Cdc16 (TBC) domain, a common structure found in most of Rab GAPs, and a TBC-Lysin motif (LysM)-Domain catalytic domain [18-20]. Mutations in the *TBC1D24* gene cause neurological disorders [21] and accumulating evidence supports that TBC1D24 is involved in neuronal development and synaptic endocytic vesicle trafficking. TBC1D24 binds to Arf6, through which TBC1D24 regulates

neuronal migration and maturation in a mouse model [22,23]. Skywalker, the *Drosophila melanogaster* homologue of TBC1D24, exhibits *in vitro* GAP activity toward Rab35 and regulates synaptic endocytic vesicle trafficking through Rab35 [24]. In addition to neuronal functions, TBC1D24 promotes breast carcinoma cell proliferation, migration, and invasion [25]. However, a molecular function of TBC1D24 is still unclear.

In the present study, we investigated the role of TBC1D24 in CIE cargo trafficking and show that TBC1D24 promotes recycling of CIE cargo proteins back to the plasma membrane through the regulation of TRE formation in HeLa cells. We also find that TBC1D24 binds to the small GTPase Rab22A, through which TBC1D24 regulates TRE-mediated CIE cargo recycling.

Materials and Methods

Antibodies. Mouse monoclonal anti-human MHCI and CD98 antibodies were purchased from Biolegend (San Diego, CA), chicken anti-GFP antibody was from Merk (Kenilworth, NJ), rabbit anti-Myc antibody was from MBL (Tokyo, Japan), and rabbit anti-FLAG and -actin antibodies were from SIGMA (Missouri, US). Rabbit anti-GFP, -Rab22A and -TBC1D24 antibodies were obtained from MBL (Tokyo, Japan), Proteintech (Chicago, IL) and Aviva System Biology (San Diego, CA), respectively. All Alexa Fluor-conjugated secondary antibodies were purchased from Invitrogen Molecular Probes (Grand Island, NY).

Plasmids. To construct plasmids for Myc-TBC1D24 and FLAG-TBC1D24, TBC1D24 cDNA was amplified by RT-PCR from total RNA prepared from HeLa cells, and inserted into pcDNA3 containing Myc-tag sequence for Myc-TBC1D24 and FLAG-tag sequence for FLAG-TBC1D24. GFP-Rab22A, GFP-Rab5A, and their constitutively active and dominant negative mutants are generous gifts from Dr. Julie G Donaldson (NHLBI, NIH).

Cell culture and transient transfection of plasmid DNAs and siRNAs. HeLa cells and HEK293T cells were cultured in Dulbecco's Modified Eagle Medium (DMEM) containing 4.5 g/l glucose and 2 mM glutamine (Nacalai tesque, Kyoto, Japan), supplemented with 10% fetal bovine serum (FBS; Life Technologies, Grand Island, NY) and 1% Penicillin/Streptomycin (Nacalai tesque), and grown under a 5% CO_2 atmosphere at 37°C. Cells were transfected with plasmid DNA or siRNA using Lipofectamine 2000 (Life Technologies) or Polyethylenimine Max (COSMO Bio, Tokyo, Japan) according to manufacturers' instructions.

Assessment for trafficking of endocytic cargo proteins. HeLa cells seeded on glass coverslips were incubated with anti-human MHCI or CD98 antibodies, or Transferrin (Tf)-Alexa Fluor 488 (Tf-488) in DMEM supplemented with 10% FBS for 30 min at 37°C to allow cells to uptake antibodies or Tf-488-Transferrin receptor (TfR) complexes. Antibodies and Tf-488 remained on the cell surface were removed by washing cells with the acid wash solution (0.5% acetic acid, 0.5 M NaCl) for 30 sec at room temperature. Cells were rinsed

with phosphate-buffered saline (PBS), fixed for 10 min in 2% formaldehyde in PBS, blocked in the blocking buffer (10% FBS and 0.02% sodium azide in PBS), and incubated with primary antibodies in PBS containing 10% FBS with 0.2% saponin. Alexa Fluor-conjugated secondary antibodies were used to detect the primary antibodies. All images were obtained using the confocal microscope TCS-SP5 (Leica Microsystems, Wetzlar, Germany) or the fluorescence microscope Axio observer Z1 (Zeiss, Thornwood, NY).

Immunoprecipitation. HEK293T cells were transfected with plasmid DNAs and incubated for 24 h. Cells were harvested and lysed with 500 μl of lysis buffer [50 mM Tris-HCl, pH 7.5, 100 mM NaCl, 1% Triton-X100, 10% Glycerol, 5 mM $MgCl_2$, and Protease Inhibitor Cocktail (Nacalai Tesque)]. The cell lysate was centrifuged at 20,000 × g for 20 min and then the supernatant was incubated with 10 μl of ANTI-FLAG M2 Affinity Gel (SIGMA-Aldrich) at 4ºC for 2 h. The gels were washed four times with the lysis buffer without protease inhibitors, and proteins bound to the gels were eluted with the SDS-PAGE sample buffer by boiling. The eluted proteins were separated by SDS-PAGE, transferred onto a PVDF membrane and immunoblotted with the specified antibodies.

Deletion of *TBC1D24* gene. The *TBC1D24* gene was deleted in the HeLa cell line using the genomic editing technique CRISPR/Cas9 as described previously [26]. Briefly, several candidate gRNA sequences targeting exon 2 of the *TBC1D24* gene were determined using the website CRISPR direct (https://crispr.dbcls.jp/). Oligo DNAs for the respective gRNA sequences were inserted into the pX459 vector (Addgene plasmid #62988), and the cleavage efficiencies of the gRNAs toward the target sequences were examined using the pCAG-EGxxFP system (Addgene plasmid 50716) [27]. The plasmid containing the gRNA sequence 5′-CACCCTGCCTGAATGCACGCGGCG-3′ was selected according to its highest efficiency and transfected into HeLa cells using Lipofectamine 2000. *TBC1D24*-knockout cell clones were selected as described previously [26].

Immunofluorescence staining-based assay for internalization of CD98. HeLa cells seeded on coverslips were incubated with anti-CD98 antibodies for 1 h on ice. Unbound

antibodies were removed by washing cells with ice-cold PBS. For analysis of the cell surface CD98 level, a set of cells were directly subjected to fixing and staining with Alexa Fluor-conjugated secondary antibody for anti-CD98 antibody. The rest of cells were incubated with DMEM supplemented with 10% FBS at 37ºC for indicated time to allow internalization of CD98-antibody complexes. After internalization, anti-CD98 antibodies remained on the cell surface were removed and immunostained as described above. All images were obtained using the confocal microscope TCS-SP5. The CD98 signal intensity was measured using the Fiji software (NIH).

Biotin-based assay for recycling of CD98. Biotin-based recycling assay was performed as described previously [28]. Briefly, HeLa cells seeded on a collagen-coated dish were incubated with EZ-Link Sulfo-NHS-Biotin (Thermo Fisher Scientific, USA)/PBS on ice for 1 h to label surface proteins. Unbound biotin was removed by washing cells with PBS twice and quenched by washing cells with 50 mM NH_4Cl twice. Cells were then incubated with the complete medium containing 50 μM primaquine and 50 μM chloroquine, which prevent the recycling of cargo proteins and lysosomal protein degradation, respectively, at 37ºC for 30 min to allow internalization of biotin-labeled cell surface proteins. After internalization, biotin remained at the cell surface was removed by washing cells with the reducing solution [60 mM 2-Mercaptoethanesulfonate sodium (MesNa), 50 mM Tris-HCl, pH 8.6, 100 mM NaCl] at 4°C for 30 min. MesNa was quenched by adding iodoacetamide to the cells. Cells were washed 3 times with PBS and further incubated with the complete medium containing 50 μM chloroquine at 37ºC for indicated time. Cells were then treated with the reducing solution again to remove biotin from recycled proteins. Cells were harvested and lysed with the lysis buffer for 10 min at 4°C. The cell lysate was centrifuged and the supernatant was incubated with 20 μl of streptavidin beads (Thermo Scientific) for 6 h at 4°C to precipitate all biotinylated-proteins. After washing five times with the lysis buffer, proteins bound to the beads were eluted and immunoblotted as described above.

Assay to analyze cell proliferation. To assess cell proliferation, HeLa cells were placed in a 6-well plate at a concentration of 1×10^5 cells/well. After incubation for 1-3 days, viable cells were counted with a hemocytometer after trypan blue staining.

Statistical analyses. All quantified data were expressed as means ± SEM and analyzed by Student's *t*-test using Excel (Microsoft, Redmond, WA, United States) or one-way ANOVA with post hoc Tukey's or Dunnett's test using the Prism 8 software (GraphPad, San Diego, CA, United States).

Results

TBC1D24 increases CIE cargo-containing tubular recycling endosomes. To examine the involvement of TBC1D24 in CIE cargo trafficking, we analyzed the trafficking of two different types of CIE cargo proteins MHCI and CD98, which follow distinct trafficking itineraries, in HeLa cells overexpressing TBC1D24. To track their intracellular trafficking, HeLa cells were incubated with antibodies directed to extracellular portions of these cargo proteins, and the internalized antibodies were detected. In most of control cells, internalized MHCI localized to punctate structures in the cytoplasm and the perinuclear region, although a small population of cells exhibited MHCI-containing TREs (Fig. 1A). In contrast, CD98 showed more prominent localization to TREs compared to MHCI (Fig. 1B). Notably, the number of cells exhibiting TREs that contain these cargo proteins was significantly increased by the overexpression of TBC1D24 (Fig. 1A, B), suggesting that TBC1D24 enhances localization of two different types of CIE cargo proteins to TREs. Overexpression of TBC1D24 did not show obvious effects on intracellular trafficking of internalized TfR, a typical CME cargo (Supplementary Fig. 1). In addition, TfR did not enter into TREs in TBC1D24-overexpressing cells as well as in control cells. These results indicate that TBC1D24 does not affect the normal sorting of TfR and TREs increased by TBC1D24 still retain their specificities to CIE cargo proteins.

To confirm the involvement of endogenous TBC1D24 in CIE cargo trafficking, we deleted the *TBC1D24* gene in HeLa cells using the CRISPR/Cas9 system (Supplementary Fig. 2A) (hereafter the cell line is referred to as Δ*TBC1D24*). In Δ*TBC1D24* cells, formation of CD98-containing TREs was significantly impaired (Fig. 1C). This phenotype was rescued by exogenous expression of TBC1D24, confirming that the effect is due to the deletion of *TBC1D24* (Fig. 1C). Similar results were also obtained in other independent *TBC1D24*-deleted clones (data not shown). The phenotype is not the result of a simple decrease in the total amount of CD98 proteins, because the deletion of *TBC1D24* did not alter the expression level of endogenous CD98 (Supplementary Fig. 2B). Furthermore, internalization of CD98 between wild type and Δ*TBC1D24* cells did not show significant difference (Supplementary Fig. 3), suggesting that the decrease of CD98-posistive TREs in Δ*TBC1D24* cells is not caused by the reduction in incoming CD98 into the cells. Collectively, these results

demonstrate that endogenous TBC1D24 is required for cells to form CIE cargo-containing TREs.

TBC1D24 promotes recycling of CIE cargo. Since TRE is a pivotal intracellular organelle for recycling of CIE cargo proteins back to the plasma membrane [10], we next analyzed the recycling of CD98 by the biochemical biotin-labeling recycling assay [28]. Rapid recycling of biotin-labeled CD98 pooled in cells, which was represented by the decrease of an internal pool of CD98, was delayed in Δ*TBC1D24* cells compared to that in wild type cells (Fig. 2A). In addition to the recycling assay, routing of CD98 was also analyzed. Previous studies suggested that defects in recycling and/or TRE formation reroute CIE cargo proteins from TRE-mediated recycling to the degradative pathway, in which cargo proteins go through EEA1-containing endosomes [6]. Consistent with the inhibition of CD98 recycling in Δ*TBC1D24* cells, the localization of CD98 to EEA1-containing endosomes was increased in these cells (Fig. 2B), indicating that CD98 is rerouted for degradation by the deletion of *TBC1D24*. Taken together, these results support the notion that TBC1D24 promotes the recycling of CIE cargo proteins mediated by TREs.

TBC1D24 regulates CIE cargo trafficking through the small GTPase Rab22A. Various Rab family small GTPases regulate CIE and the following membrane trafficking [6,7,9-14]. Among these Rab proteins, Rab22A has been demonstrated to play critical roles in CIE cargo recycling mediated by CIE-specific TREs [10,11]. Therefore, we tested the binding of TBC1D24 to Rab22A. The immunoprecipitation assay revealed that FLAG-TBC1D24 expressed in HEK293T cells co-precipitated with co-expressed GFP-Rab22A, indicating that TBC1D24 is functionally related to Rab22A (Fig. 3A). On the other hand, TBC1D24 did not interact with Rab5A, which is involved in the maturation of EE/SE [12,13] (Fig. 3A). These results are consistent with the finding that TBC1D24 is involved in TRE-mediated recycling, the stage after the cargo exit from EE/SE.

We next investigated the functional relationship between TBC1D24 and Rab22A in the CIE cargo trafficking. Knockdown of Rab22A counteracted the increase of TREs induced by overexpression of TBC1D24 (Fig. 3B), whereas the decrease of TREs observed in

Δ*TBC1D24* cells was restored by the overexpression of Rab22A (Fig. 3C). These results indicate that TBC1D24 regulates TRE formation through Rab22A. Furthermore, the dominant negative mutant Rab22A S19N, but not the constitutively active mutant Rab22A Q64L, almost completely abolished the effect of TBC1D24 overexpression on TRE formation (Fig. 4). Taken together with the previous reports showing that the activation of Rab22A is required for TRE formation [10,11], these results suggest that TBC1D24 requires active Rab22A to regulate formation of TREs.

TBC1D24 and Rab22A regulate cell proliferation. It has been reported that CIE and following intracellular trafficking regulate the turnover of cargo proteins, including CD44, CD98 and CD147, involved in cell proliferation [6]. Given that deletion of *TBC1D24* led to a suppression of CD98 recycling, we wondered whether TBC1D24 is required for cell proliferation. To answer this question, cell proliferative capacities of wild type and Δ*TBC1D24* cells were determined. The result showed that deletion of *TBC1D24* inhibits cell proliferation (Supplementary Fig. 4A). Consistent with the finding that TBC1D24 regulates TRE formation through Rab22A, knockdown of Rab22A suppressed cell proliferation (Supplementary Fig. 4B). These observations indicate that TBC1D24-mediated recycling of CIE cargo proteins might facilitate cell proliferation.

Discussion

In the present study, we provide evidence that in HeLa cells, TBC1D24 facilitates the CIE cargo recycling mediated by TREs. We also found that TBC1D24 binds to the small GTPase Rab22A, through which TBC1D24 regulates formation of TREs. Our findings provide insights into the regulatory mechanism of TRE-mediated CIE cargo recycling.

Although the TBC domain is a common structure of multiple Rab GAPs, our findings suggest that TBC1D24 positively regulates Rab22A functions rather than functioning as a Rab22A GAP. Interestingly, TBC1D24 contains an atypical TBC domain: canonical TBC domains contain arginine and glutamine dual 'fingers' required for their GAP activities, whereas the TBC domain of TBC1D24 lacks arginine and glutamine residues that are critical for these fingers. Several TBC proteins also possess the similar atypical TBC domain, and they are indicated to have alternative functions to regulate their target proteins [29-31]. Therefore, it is likely that TBC1D24 regulates Rab22A in a GAP activity-independent manner.

The detailed mechanism of how TBC1D24 regulates Rab22A remains to be elucidated. The results obtained in this study led us to speculate that TBC1D24 directly or indirectly activates Rab22A. However, in a ^{32}P-metabolic labeling assay system, we could not observe the activation of Rab22A by the overexpression of TBC1D24 (data not shown). We therefore hypothesize that TBC1D24 recruits Rab22A to the sites where tubulation of endosome membranes initiates and/or the tubular structure is extending. It has been reported that Rab22A localizes to TREs and vesicular structures at the cell periphery [10,11]. Deletion of *TBC1D24* might disturb the localization of Rab22A to these compartments.

The findings in this study suggest that TBC1D24 contributes to the control of the amount and localization of plasma membrane proteins by facilitating the TRE-mediated recycling, thereby regulating various cellular functions. Our finding that TBC1D24 and Rab22A both promote cell proliferation (Supplementary Fig. 4) supports this notion. TBC1D24 has been reported to be related to oncogenesis and neurological disorders. Therefore, identification of TBC1D24-dependent cargo proteins related to these diseases and investigation of how their trafficking is regulated by TBC1D24 would provide insights into mechanisms for the pathogenesis of TBC1D24-related diseases.

Acknowledgement

We thank Dr. Y. Watanabe (University of Tsukuba) for the technical support on generating *TBC1D24*-knockout cells by the CRISPR/Cas9 method. We are grateful to Dr. J. G. Donaldson (NHLBI, NIH) for generous gifts of GFP-Rab22A plasmids. This work is supported by the Ministry of Education, Culture, Sports, and Technology (MEXT) of Japan (KAKENHI, 18H02601 to YK, 19K06653 to NO, and 17K07327 to YF).

Author contributions

NTKN acquired, analyzed, interpreted data, and designed study; YF and YK analyzed, interpreted data, and designed study; NTKN, YF and YK drafted manuscript; NO technically supported for this study and interpreted data; all authors reviewed final manuscript.

Supplementary data

Supplementary data accompany this paper.

Conflict of interest

The authors listed declare no conflict of interests regarding this study.

References

[1] K. Sandvig, S. Kavaliauskiene, T. Skotland, Clathrin-independent endocytosis: an increasing degree of complexity, Histochem Cell Biol 150 (2018) 107-118.

[2] M. Kaksonen, A. Roux, Mechanisms of clathrin-mediated endocytosis, Nat Rev Mol Cell Biol 19 (2018) 313-326.

[3] N. Naslavsky, R. Weigert, J.G. Donaldson, Characterization of a nonclathrin endocytic pathway: membrane cargo and lipid requirements, Mol Biol Cell 15 (2004) 3542-3552.

[4] L. Maldonado-Baez, C. Williamson, J.G. Donaldson, Clathrin-independent endocytosis: a cargo-centric view, Exp Cell Res 319 (2013) 2759-2769.

[5] S. Mayor, R.G. Parton, J.G. Donaldson, Clathrin-independent pathways of endocytosis, Cold Spring Harb Perspect Biol 6 (2014).

[6] L. Maldonado-Baez, N.B. Cole, H. Kramer, J.G. Donaldson, Microtubule-dependent endosomal sorting of clathrin-independent cargo by Hook1, J Cell Biol 201 (2013) 233-247.

[7] L. Maldonado-Baez, J.G. Donaldson, Hook1, microtubules, and Rab22: mediators of selective sorting of clathrin-independent endocytic cargo proteins on endosomes, Bioarchitecture 3 (2013) 141-146.

[8] C.A. Eyster, J.D. Higginson, R. Huebner, N. Porat-Shliom, R. Weigert, W.W. Wu, R.F. Shen, J.G. Donaldson, Discovery of new cargo proteins that enter cells through clathrin-independent endocytosis, Traffic 10 (2009) 590-599.

[9] H. Radhakrishna, J.G. Donaldson, ADP-ribosylation factor 6 regulates a novel plasma membrane recycling pathway, J Cell Biol 139 (1997) 49-61.

[10] R. Weigert, A.C. Yeung, J. Li, J.G. Donaldson, Rab22a regulates the recycling of membrane proteins internalized independently of clathrin, Mol Biol Cell 15 (2004) 3758-3770.

[11] S. Shakya, P. Sharma, A.M. Bhatt, R.A. Jani, C. Delevoye, S.R. Setty, Rab22A recruits BLOC-1 and BLOC-2 to promote the biogenesis of recycling endosomes, EMBO Rep 19 (2018).

[12] M. Jovic, M. Sharma, J. Rahajeng, S. Caplan, The early endosome: a busy sorting station for proteins at the crossroads, Histol Histopathol 25 (2010) 99-112.

[13] J. Huotari, A. Helenius, Endosome maturation, EMBO J 30 (2011) 3481-3500.

[14] S. Xie, K. Bahl, J.B. Reinecke, G.R. Hammond, N. Naslavsky, S. Caplan, The endocytic recycling compartment maintains cargo segregation acquired upon exit from the sorting endosome, Mol Biol Cell 27 (2016) 108-126.
[15] J.L. Bos, H. Rehmann, A. Wittinghofer, GEFs and GAPs: critical elements in the control of small G proteins, Cell 129 (2007) 865-877.
[16] M.P. Muller, R.S. Goody, Molecular control of Rab activity by GEFs, GAPs and GDI, Small GTPases 9 (2018) 5-21.
[17] J. Cherfils, M. Zeghouf, Regulation of small GTPases by GEFs, GAPs, and GDIs, Physiol Rev 93 (2013) 269-309.
[18] M.A. Frasa, K.T. Koessmeier, M.R. Ahmadian, V.M. Braga, Illuminating the functional and structural repertoire of human TBC/RABGAPs, Nat Rev Mol Cell Biol 13 (2012) 67-73.
[19] M.J. Finelli, L. Sanchez-Pulido, K.X. Liu, K.E. Davies, P.L. Oliver, The Evolutionarily Conserved Tre2/Bub2/Cdc16 (TBC), Lysin Motif (LysM), Domain Catalytic (TLDc) Domain Is Neuroprotective against Oxidative Stress, J Biol Chem 291 (2016) 2751-2763.
[20] M.J. Finelli, P.L. Oliver, TLDc proteins: new players in the oxidative stress response and neurological disease, Mamm Genome 28 (2017) 395-406.
[21] M.A. Corbett, M. Bahlo, L. Jolly, Z. Afawi, A.E. Gardner, K.L. Oliver, S. Tan, A. Coffey, J.C. Mulley, L.M. Dibbens, W. Simri, A. Shalata, S. Kivity, G.D. Jackson, S.F. Berkovic, J. Gecz, A focal epilepsy and intellectual disability syndrome is due to a mutation in TBC1D24, Am J Hum Genet 87 (2010) 371-375.
[22] A. Falace, F. Filipello, V. La Padula, N. Vanni, F. Madia, D. De Pietri Tonelli, F.A. de Falco, P. Striano, F. Dagna Bricarelli, C. Minetti, F. Benfenati, A. Fassio, F. Zara, TBC1D24, an ARF6-interacting protein, is mutated in familial infantile myoclonic epilepsy, Am J Hum Genet 87 (2010) 365-370.
[23] A. Falace, E. Buhler, M. Fadda, F. Watrin, P. Lippiello, E. Pallesi-Pocachard, P. Baldelli, F. Benfenati, F. Zara, A. Represa, A. Fassio, C. Cardoso, TBC1D24 regulates neuronal migration and maturation through modulation of the ARF6-dependent pathway, Proc Natl Acad Sci U S A 111 (2014) 2337-2342.

[24] V. Uytterhoeven, S. Kuenen, J. Kasprowicz, K. Miskiewicz, P. Verstreken, Loss of skywalker reveals synaptic endosomes as sorting stations for synaptic vesicle proteins, Cell 145 (2011) 117-132.
[25] X. Qu, B. Zhao, M. Hu, Z. Ji, J. Xu, W. Xia, Y. Qu, Downregulation of TBC1 Domain Family Member 24 (BC1D24) Inhibits Breast Carcinoma Growth via IGF1R/PI3K/AKT Pathway, Med Sci Monit 24 (2018) 3987-3996.
[26] F.A. Ran, P.D. Hsu, J. Wright, V. Agarwala, D.A. Scott, F. Zhang, Genome engineering using the CRISPR-Cas9 system, Nat Protoc 8 (2013) 2281-2308.
[27] S. Mizuno, T.T. Dinh, K. Kato, S. Mizuno-Iijima, Y. Tanimoto, Y. Daitoku, Y. Hoshino, M. Ikawa, S. Takahashi, F. Sugiyama, K. Yagami, Simple generation of albino C57BL/6J mice with G291T mutation in the tyrosinase gene by the CRISPR/Cas9 system, Mamm Genome 25 (2014) 327-334.
[28] M. Roberts, S. Barry, A. Woods, P. van der Sluijs, J. Norman, PDGF-regulated rab4-dependent recycling of alphavbeta3 integrin from early endosomes is necessary for cell adhesion and spreading, Curr Biol 11 (2001) 1392-1402.
[29] E. Frittoli, A. Palamidessi, A. Pizzigoni, L. Lanzetti, M. Garre, F. Troglio, A. Troilo, M. Fukuda, P.P. Di Fiore, G. Scita, S. Confalonieri, The primate-specific protein TBC1D3 is required for optimal macropinocytosis in a novel ARF6-dependent pathway, Mol Biol Cell 19 (2008) 1304-1316.
[30] L. Martinu, J.M. Masuda-Robens, S.E. Robertson, L.C. Santy, J.E. Casanova, M.M. Chou, The TBC (Tre-2/Bub2/Cdc16) domain protein TRE17 regulates plasma membrane-endosomal trafficking through activation of Arf6, Mol Cell Biol 24 (2004) 9752-9762.
[31] C. Bizimungu, M. Vandenbol, At least two regions of the oncoprotein Tre2 are involved in its lack of GAP activity, Biochem Biophys Res Commun 335 (2005) 883-890.

Figure legends

Fig. 1. TBC1D24 promotes formation of tubular recycling endosomes loaded with CIE cargo proteins. (A, B) HeLa cells were transfected with control or Myc-TBC1D24 plasmid. After 24 h, cells were incubated with antibodies specific to MHCI (A) and CD98 (B) for 30 min. Surface antibodies were removed and the cargo protein-antibody complexes internalized into cells were detected by secondary antibodies. The number of cells exhibiting MHCI- or CD98-positive TREs was counted and expressed as the percentage of transfected cells. (C) Wild type and *ΔTBC1D24* cells were transfected with control or Myc-TBC1D24 plasmid, and CD98-containing TREs were observed as in (B). Arrowheads indicate the cells with CD98-containing TREs. All the graphs shown are means ± SEM from three independent experiments. ***$p < 0.001$, Student's *t*-Test for (A) and (B); *$p < 0.05$, **$p < 0.005$, one-way ANOVA with post hoc Tukey's multiple comparison test for (C). All scale bars, 10 μm.

Fig. 2. Deletion of *TBC1D24* inhibits recycling of CD98 and alters the trafficking of CD98. (A) Recycling of CD98 was quantitated in wild type and *ΔTBC1D24* cells by the biotin-based recycling assay. Intracellular CD98 pools remaining at the indicated time points were quantified, and recycled CD98 was calculated. Recycling rates were expressed as percentage of the initial intracellular pool of CD98 (0 min). (B) Subcellular localization of internalized CD98 was observed in wild type and *ΔTBC1D24* cells as in Fig. 1B (green). Cells were also stained with the antibody specific to EEA1 (red). Enlargements of the boxed regions are shown in the insets. Dashed lines indicate the outline of the cells. Scale bars, 10 μm. Colocalization of CD98 and EEA1 was quantified by the Pearson correlation coefficient using the Fiji software. All the quantified data shown are means ± SEM from three independent experiments. *$p < 0.05$; n.s., not significant, Student's *t*-Test.

Fig. 3. TBC1D24 regulates CIE cargo trafficking through Rab22A. (A) HEK293T cells were transfected with control or FLAG-TBC1D24 plasmid and GFP-Rab22A or GFP-Rab5A plasmid. Cells were subjected to the immunoprecipitation assay, and the proteins were detected by immunoblotting using specified antibodies. (B) HeLa cells treated with control

or Rab22A-specific siRNA were transfected with either control or Myc-TBC1D24 plasmid. CD98-containing TREs were observed as in Fig. 1B. The knockdown efficiency of siRNA for Rab22A was assessed by immunoblotting. (C) Wild type and *ΔTBC1D24* HeLa cells were transfected with either GFP or GFP-Rab22A plasmid. CD98-containing TREs were observed as in Fig. 1B. Arrowheads indicate the cells with CD98-containing TREs. The graphs shown represent means ± SEM from three independent experiments. *$p < 0.05$, ***$p < 0.001$, ****$p < 0.0001$; n.s., not significant, one-way ANOVA with post hoc Dunnett's multiple comparison test for (B) and post hoc Tukey's multiple comparison test for (C). Scale bars, 10 μm.

Fig. 4. Active Rab22A is required for TBC1D24 to promote TRE formation. HeLa cells were transfected with control or FLAG-TBC1D24 plasmid with or without GFP-Rab22A Q64L or S19N. CD98-containing TREs were observed as in Fig. 1B. Arrowheads indicate the cells with CD98-containing TREs. The graph represents means ± SEM from three independent experiments. ****$p < 0.0001$; n.s., not significant, one-way ANOVA with post hoc Tukey's multiple comparison test. Scale bars, 10 μm.

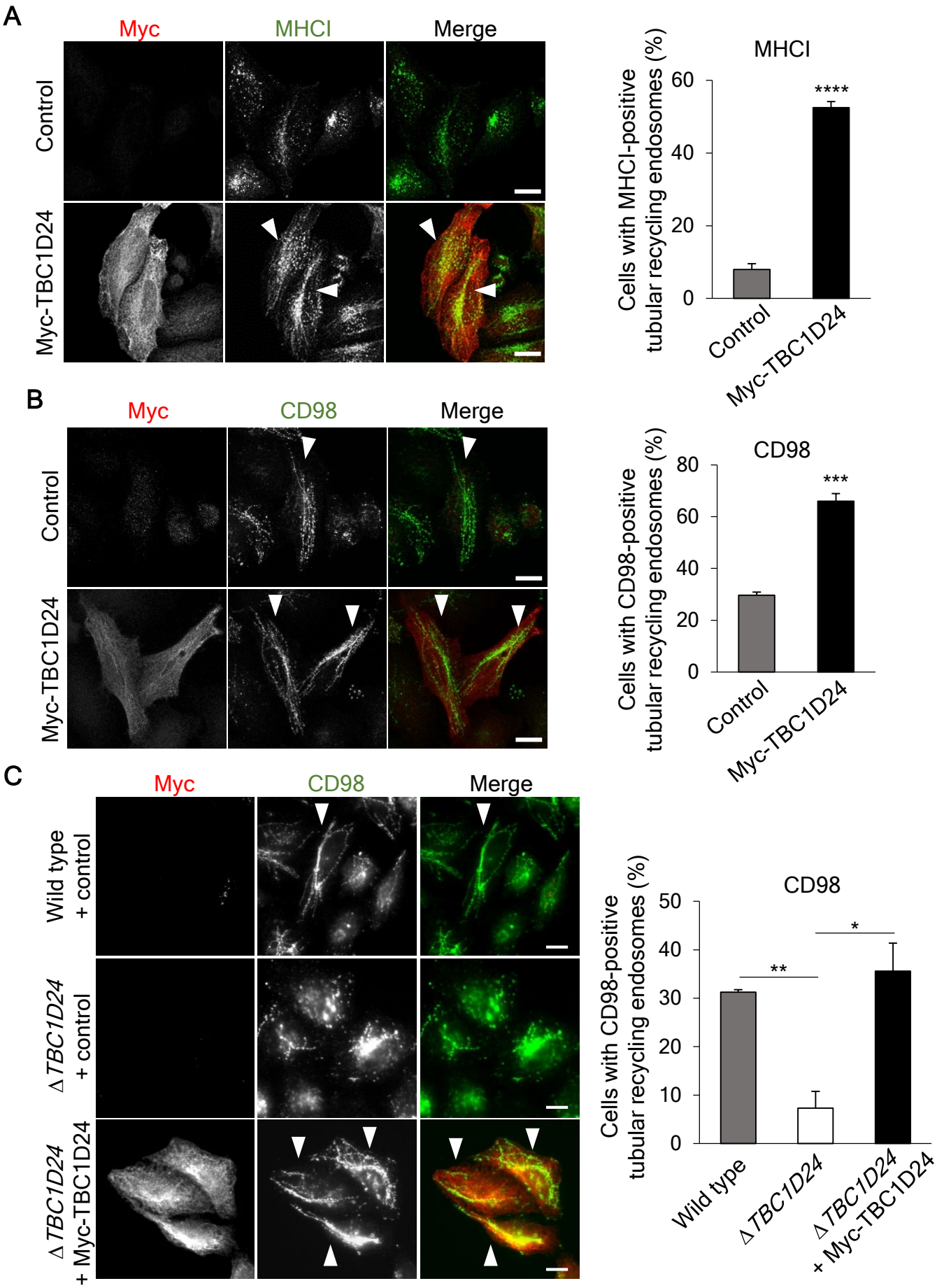

Fig. 1 N.T. K. Nguyen

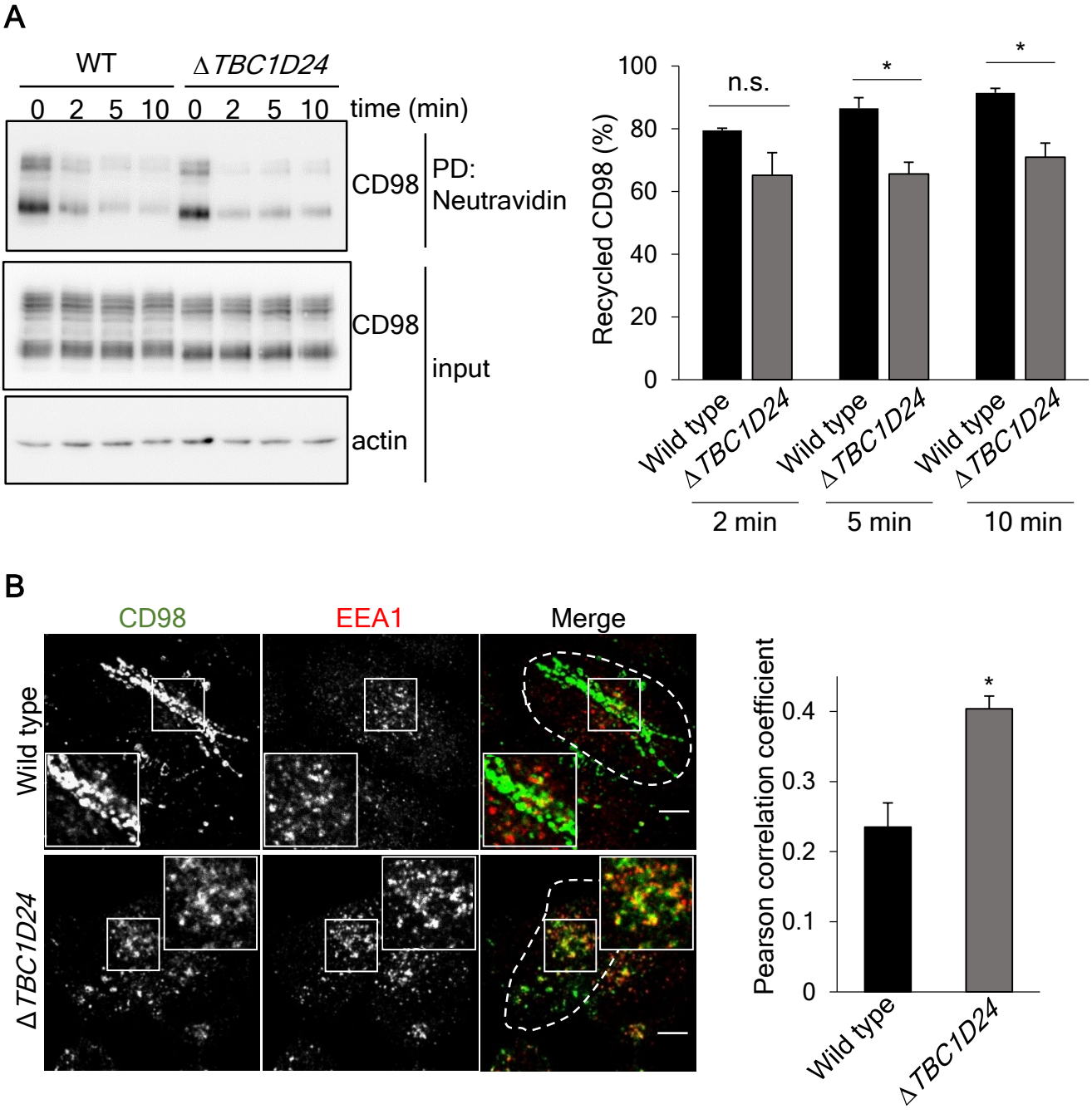

Fig. 2 N.T. K. Nguyen

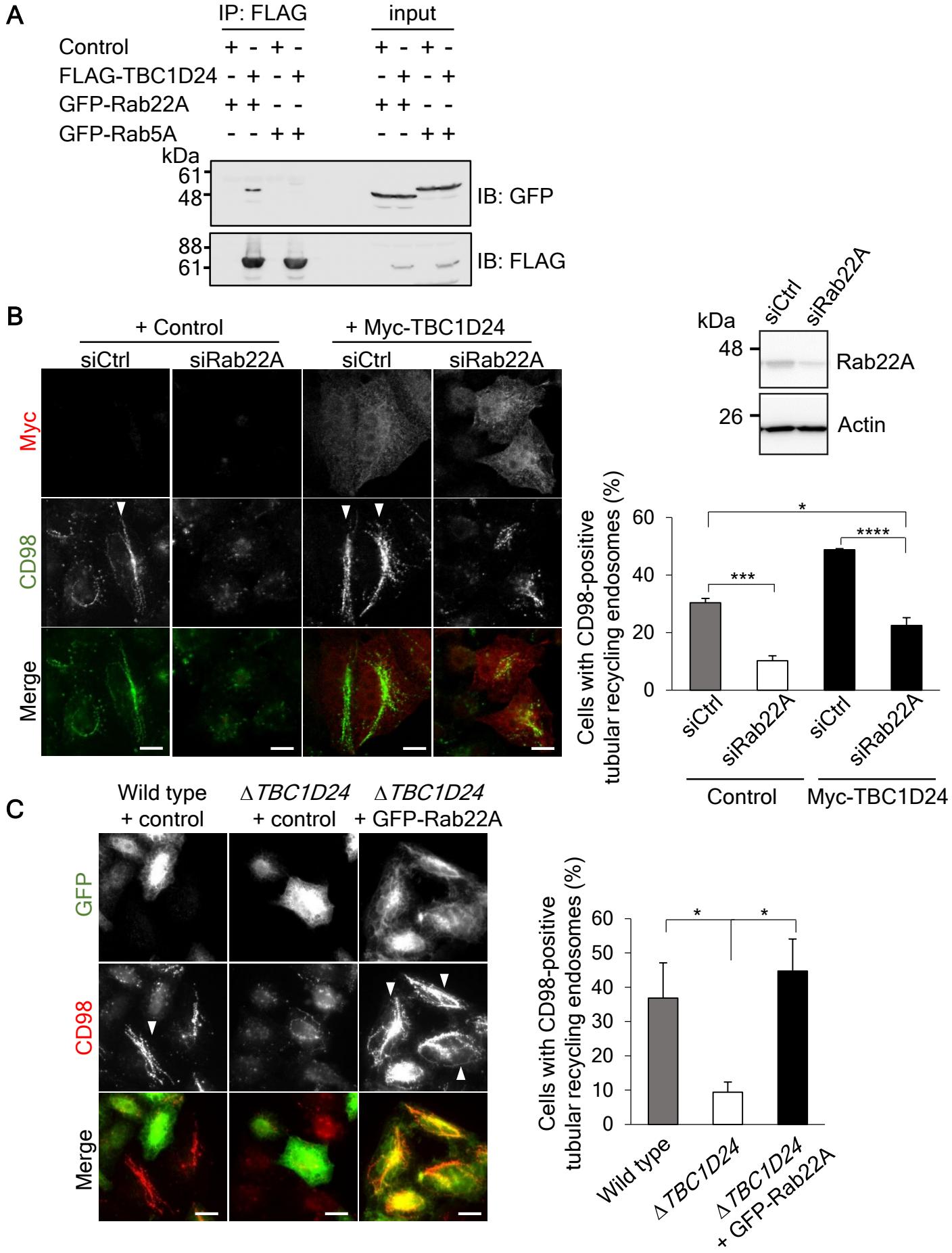

Fig. 3 N.T. K. Nguyen

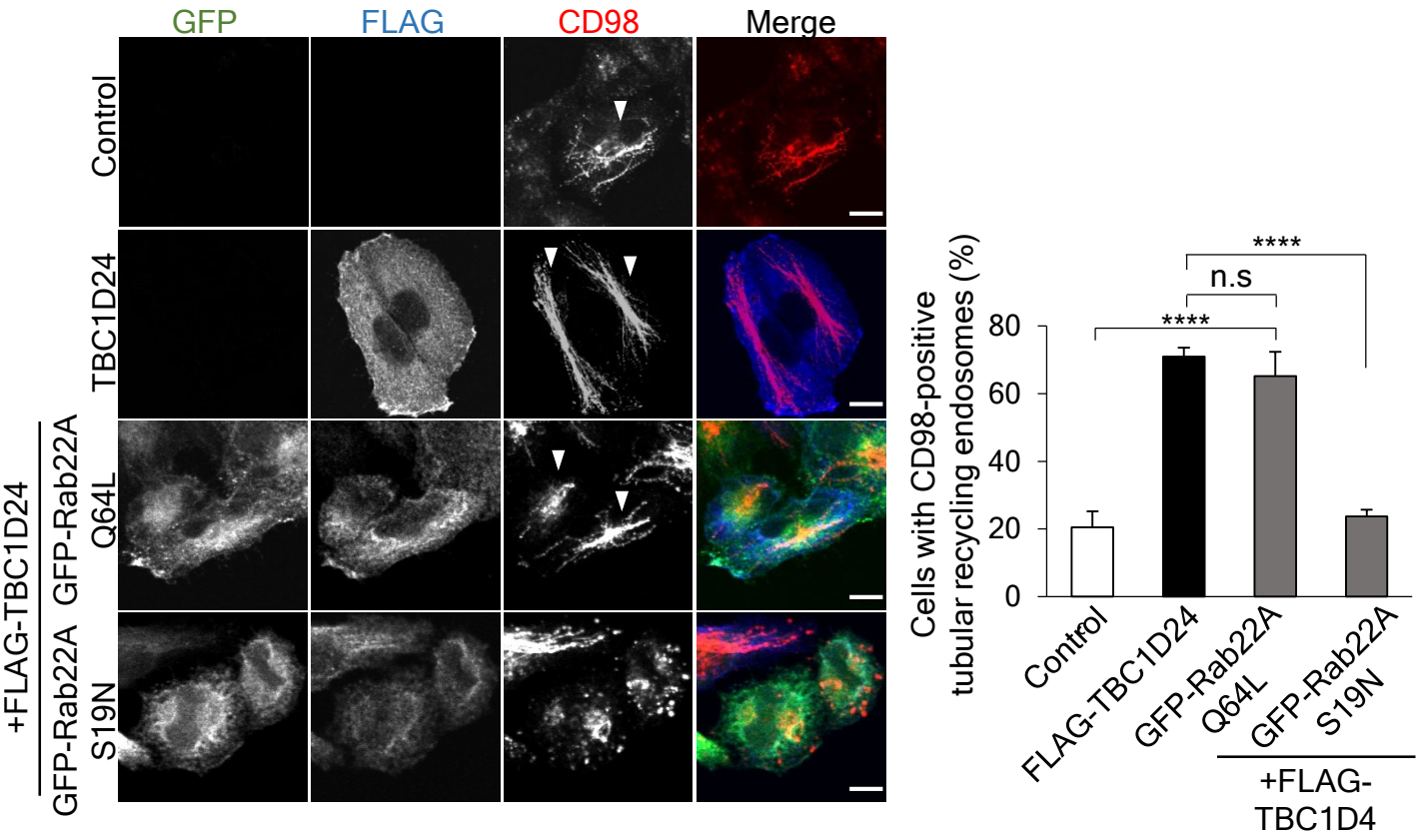

Fig. 4 N.T. K. Nguyen

Supplementary Figures

TBC1D24 regulates recycling of clathrin-independent cargo proteins mediated by tubular recycling endosomes

Nguyen Thi Kim Nguyen, Norihiko Ohbayashi,
Yasunori Kanaho, Yuji Funakoshi

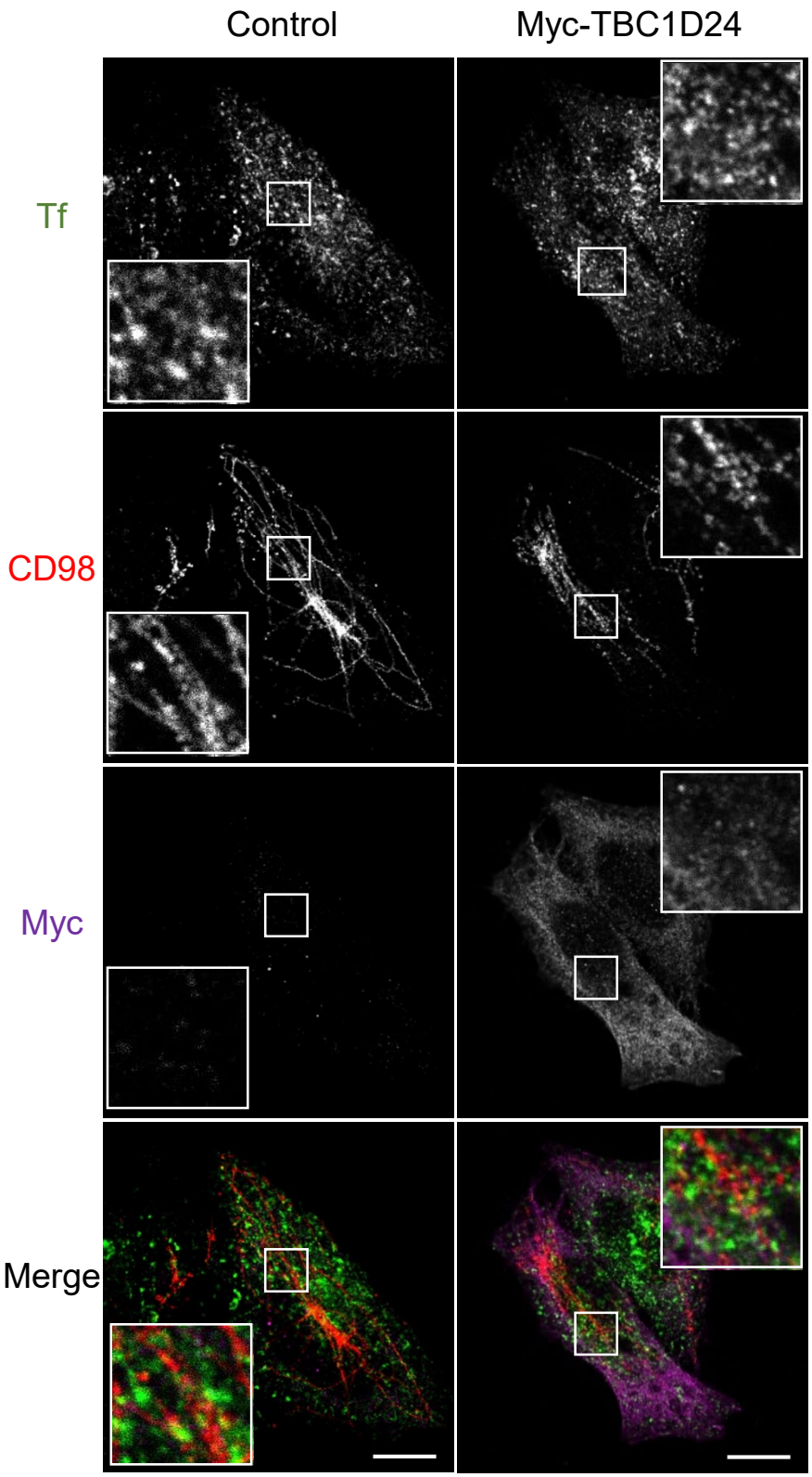

Supplementary Fig. 1. TBC1D24 does not affect the localization of the CME cargo protein TfR. Hela cells were transfected with control or Myc-TBC1D24 plasmid, and cultured for 24 h. The cells were incubated with CD98 antibodies and Tf-Alexa488 for 30 min to allow internalization of the cargo proteins. Surface antibodies and Tf-Alexa488 were removed as described in Materials and Methods. CD98-antibody complexes were detected with secondary antibodies. Enlargements of the boxed regions are shown in the insets. Scale bar, 10 μm.

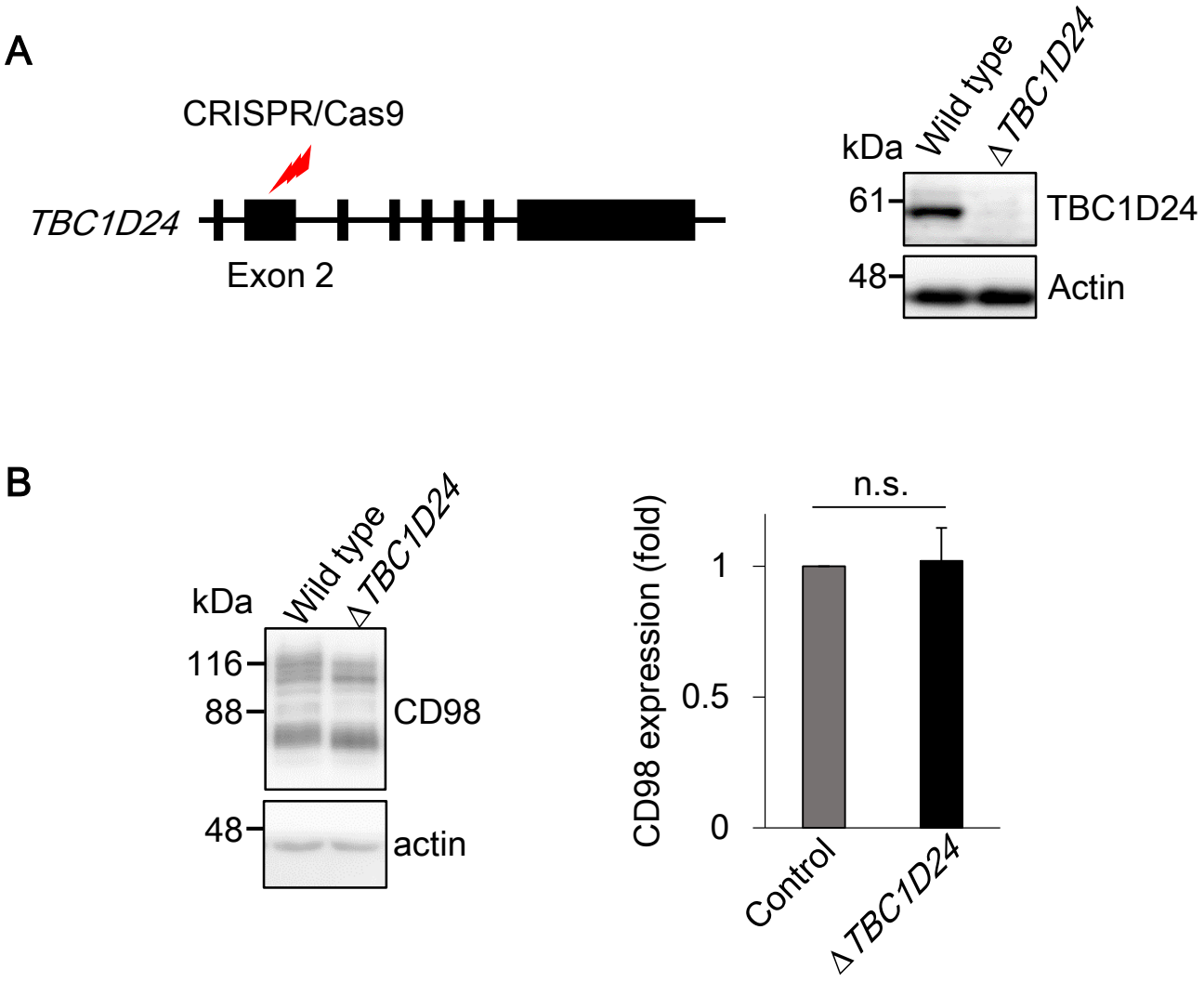

Supplementary Fig. 2. Generation of *TBC1D24* knockout cell clone using the CRISPR/Cas9 system. (A) Schematic representation of the *TBC1D24* gene and the CRISPR-Cas9 target site in the exon 2 (left). Expression of TBC1D24 in wild type cells and the TBC1D24 knockout cell clone was assessed by immunoblotting using the anti-human TBC1D24 antibody (right). (B) Whole cell lysates of wildtype and Δ*TBC1D24* cells were subjected to immunoblotting using antibodies to CD98 and β-actin. Signal intensities of immunoblotted bands were measured. The graph represents means ± SEM from three independent experiments. n.s., not significant, Student's *t*-Test.

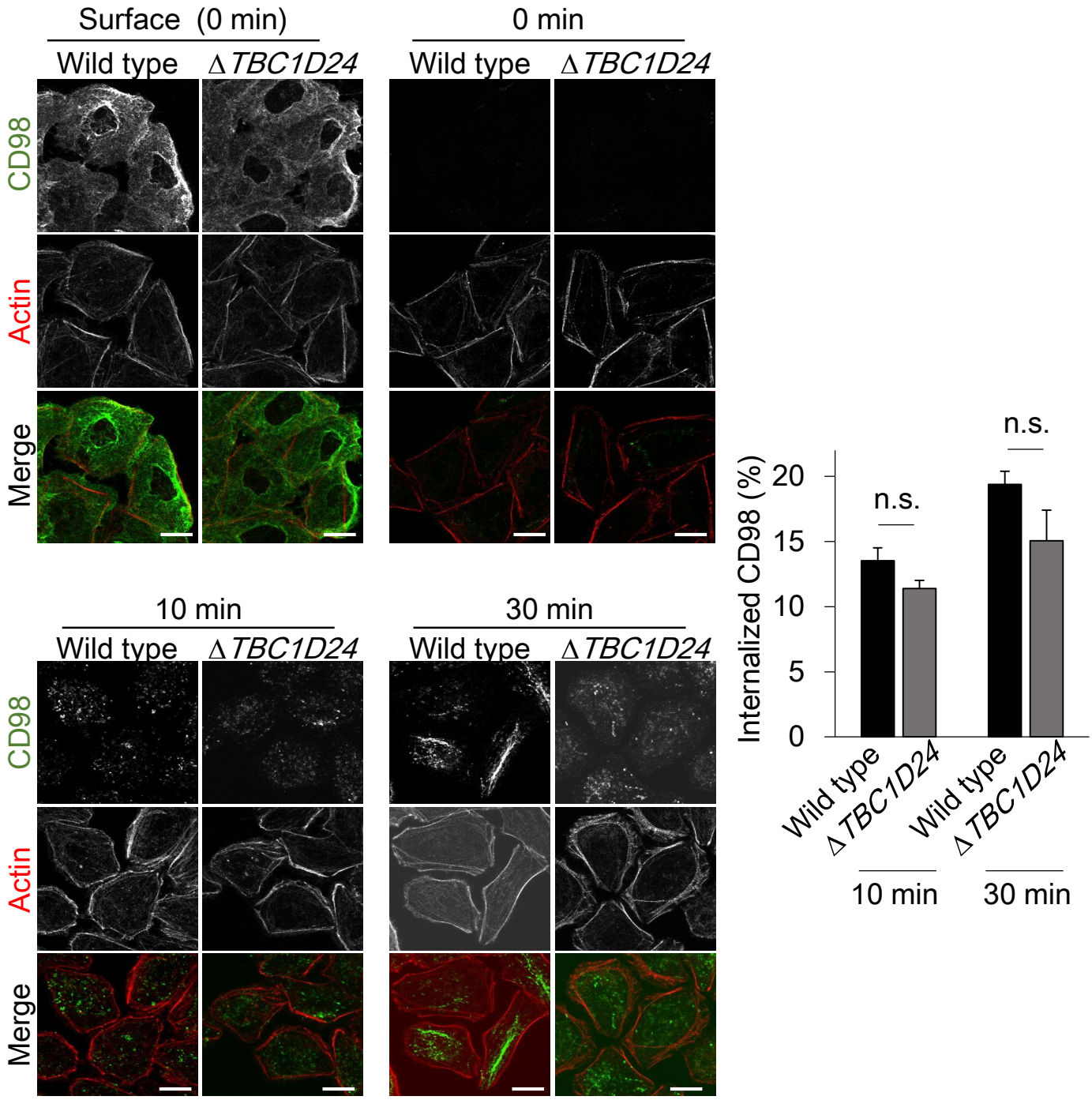

Supplementary Fig. 3. Internalization of CD98 is not affected by the deletion of *TBC1D24*. Wild type and Δ*TBC1D24* cells were incubated with anti-CD98 antibodies on ice for 1 h to label the surface CD98. A set of cells were directly fixed and stained with secondary antibodies without saponin to stain the surface CD98 (surface). Rest of cells were incubated at 37°C for the indicated time to allow internalization of CD98 proteins. Surface antibodies were removed, and the CD98-antibody complexes internalized into cells were detected by secondary antibodies in the presence of saponin. Scale bars, 10 μm. The graph represents means ± SEM from three independent experiments. n.s., not significant, Student's *t*-Test.

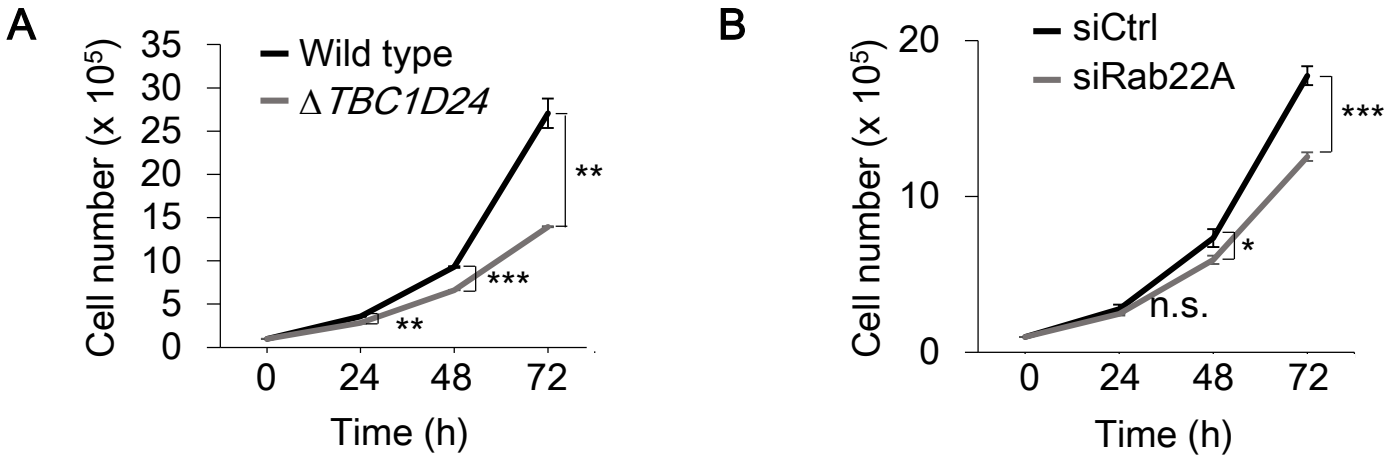

Supplementary Fig. 4. TBC1D24 and Rab22A regulate cell proliferation. (A) Wild type and *ΔTBC1D24* cells were seeded on dishes and kept culturing for the indicated time. At the each time point, cells were collected and the cell number was counted using hemocytometer. (B) HeLa cells were transfected with control (siCtrl) or Rab22A-specific siRNA (siRab22A). After 24 h, cells were re-seeded on new dishes, cultured and their cell number was counted as in (A). The graphs represent means ± SEM from three independent experiments. *$p < 0.05$, **$p < 0.01$, ***$p < 0.001$, Student's *t*-Test.